RESEARCH ARTICLE

Innovation in Practice

A novel method for estimating avian roost sizes using passive acoustic recordings using deep neural network

Malcolm C. K. Soh[1] | **Mandar A. Chitre**[2] | **Matthias Hoffmann-Kuhnt**[2] |
Benjamin P. Y.-H. Lee[1] | **Kenneth B. H. Er**[1]

[1]National Parks Board, Singapore, Singapore

[2]Acoustic Research Laboratory, National University of Singapore, Tropical Marine Science Institute, Singapore, Singapore

Correspondence
Mandar A. Chitre
Email: mandar@nus.edu.sg

Abstract

1. Communal bird roosts serve as information centres and a means of thermoregulation for many species. While some communally roosting species are major pests and cause dis-amenities, others are of conservation concern. Estimating the population of roosting birds can provide a useful proxy of population size and possibly a more reliable estimate than other sampling techniques. However, estimating these populations is challenging as some roosts are large and often occluded in foliage.

2. Previous acoustic methods such as paired sampling, microphone arrays and use of call rate have been used to estimate bird abundances; however, these are less suited for estimating large roost populations where hundreds of individuals are calling in unison. To address this challenge, we explored using machine learning techniques to estimate a roost population of the Javan myna, *Acridotheres javanicus*, an invasive species in Singapore. While one may expect to use sound intensity to estimate roost sizes, it is affected by various factors such as distance to the recorder, local propagation conditions (e.g. buildings and trees), weather conditions, and noise from other sources. Here, we used a deep neural network to extract higher order statistics from the sound recordings and use those to help estimate roost sizes. Additionally, we validated our method using automated visual analysis with a dual-camera setup and manual bird counts.

3. Our estimated bird counts over time using our acoustic model matched the automated visual estimates and manual bird counts at a selected Javan myna roost, thus validating our approach. Our acoustic model estimated close to 400 individual mynas roosting in a single tree. Analyses of additional recordings of Javan myna roosts conducted on two separate occasions and at a different roost location using our acoustic model showed that our roost estimates over time also matched our automated visual estimates well.

4. Practical implication: Our novel approach of estimating communal roost sizes can be achieved robustly using a simple portable acoustic recording system. Our method has multiple applications such as testing the efficacy of avian

roost population control measures (e.g. roost tree pruning) and monitoring the populations of threatened bird species that roost communally.

1 | INTRODUCTION

Communal bird roosts are prevalent in several avian families (Beauchamp, 1999). They serve to provide protection and safety in numbers against predators (Goodenough et al., 2017), provide thermoregulatory benefits against extreme climatic conditions (Brodsky & Weatherhead, 1984; Merola-Zwartjes, 1998) and operate as information centres where knowledge on foraging sites for example could be transmitted among members (Marzluff et al., 1996; Ward & Zahavi, 1973).

Some undesirable species can form large roosts. The red-winged blackbird (*Agelaius phoeniceus*) can depredate up to 360,000 tonnes of corn in North America annually in farms near their roosts (Dolbeer, 1990). The red-billed quelea (*Quelea quelea*) is a widespread migratory pest in Africa, depredating grain crops such as millet, wheat and rice, and causing an economic loss of approximately US$ 90 million per annum (Cheke & El Hady Sidatt, 2019). Communally roosting birds can also cause infrastructural damage in urban areas. Feral pigeon (*Columba livia*) droppings are corrosive and can damage bridges, walkways and buildings including those of historical significance (Giunchi et al., 2012; Haag-Wackernagel & Geigenfeind, 2008). Inhalation of *Cryptococcus neoformans* or *Histoplasma capsulatum* fungal spores in dried excreta of communal roosters can also cause lung ailments and may be fatal in rare instances (Deepe Jr., 2018; Denton & Di Salvo, 1968; Gurney & Conces, 1996; Malik et al., 2003). The likelihood of bird-strikes at airports also increases if there are nearby communal roosts of birds (Burger, 1983).

Conversely, some species that roost communally are threatened. Many parrot species roost communally and more than a third are threatened from habitat loss or poaching for the pet trade (IUCN, 2022). For the critically endangered yellow-naped parrot (*Amazona auropalliata*) and endangered vinaceous-breasted parrot (*Amazona vinacea*), roost counts provide a useful means of monitoring their populations (Matuzak & Brightsmith, 2007; Zulian et al., 2020).

Given the prevalence of communally roosting birds, estimating roost populations reliably can guide the management of bird commensals and species of conservation concern. For such species, roost counts provide a more accurate population estimate than other sampling techniques such as point counts or line transects, as individual birds tend to be sparsely distributed or constantly on the move (e.g. aerial feeders including swifts and swallows) when not in roost. Roost populations tracked over time can also provide

a clearer understanding of their phenology. A study revealed that yellow-crested cockatoos (*Cacatua sulphurea*) regularly switch roost sites depending on prevailing microclimatic conditions (Wang & Chu, 2021). Over the course of 20 years, pre-migration roosting populations of swallows and martins have displayed a tendency to shift earlier, a change likely attributed to climate change (Deng et al., 2023). This shift implies that these birds had inadequate time to accumulate sufficient food resources to support their upcoming migration. Common starlings (*Sturnus vulgaris*), a bird commensal species in Washington, USA, have been found to gather in dairies to roost closer to late fall, winter, and early spring. Such information could prompt farmers then to deter these birds from forming roosts and lessen the likelihood of their excreta mixing with cattle feed and spreading disease (Lichtenwalter et al., 2023).

However, performing accurate visual counts of birds roosting can be challenging (Gregory et al., 2004; van Els & van Turnhout, 2021). Birds that form large roosts in dense canopies are often occluded in foliage or by other individuals. Aerial and even satellite photos of roosts are alternatives, but are limited to larger species and obstructed views persist for densely populated roosts (Chabot & Francis, 2016). Visually tracking flocks of birds as they return to their roost can also be confusing since individuals often move in and out of their roost prior to eventually settling in. The mere presence of surveyors may further bias counts as some species or individuals may feel threatened. Additionally, detecting birds after they have settled in their roosts can be difficult since it usually occurs past sunset and is dark. Furthermore, even daily estimates can be highly variable and several repeated counts are needed (Cougill & Marsden, 2004). Weather radar had been used for estimating roost populations of swallows, martins, blackbirds and American robins (*Turdus migratorius*), but this approach is more suited for larger roosts, usually numbering a hundred thousand or more individuals (Clark et al., 2020; Russell & Gauthreaux, 1998; Van Den Broeke, 2019).

Given the associated biases with visual or radar estimates of abundance or density, researchers have also explored acoustic methods to improve accuracy (Yip et al., 2020). Paired sampling, where human observers conduct surveys synchronously with acoustic recorders, apply a correction factor to account for their different detection radii (Bombaci & Pejchar, 2019; Van Wilgenburg et al., 2017). The correction factors are then used in generalized linear models to help reduce biases between ARUs and traditional point counts. Nonetheless, precise distances of the bird to the recorder can be difficult to attain for elusive species particularly

FIGURE 1 (a) Two roost sites chosen in Singapore for data collection. Roost site 1 was the primary target for visual and acoustic data collection. Roost site 2 had no clear view for visual data analysis, but was used for acoustic data analysis. Illustrative projections of the microphone beamwidth and virtual markers for Cameras 1 and 2 depicted in orange dotted lines, and blue and red frames respectively. Sample video frames showing birds detected in yellow boxes on Camera 1 (b) and Camera 2 (c) while flying in and out of the roost site.
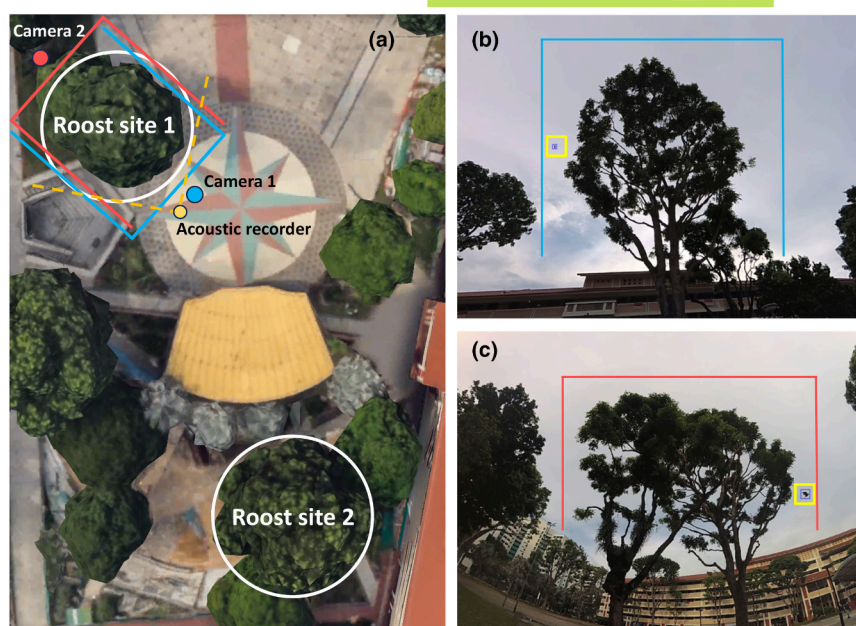
TABLE 1 Data collected for training and validating the acoustic model and validating the visual counts.

Date	Data type		Purpose			Remarks
	Audio	Visual	Training (acoustic)	Validation (visual)	Validation (acoustic)	
3 September 2020	✓	✓	✓	✓	—	
17 February 2021	✓	✓	—	—	✓	Primary data for validation
20 August 2020	✓	✓	—	—	✓	Only 18 min of audio recorded
31 August 2020	✓	Partial	—	—	—	Nearby vegetation occluded roost tree
5 February 2021	✓	✓	—	—	✓	Wind cover used

in densely forested habitats (Pérez-Granados & Traba, 2021). Microphone arrays in the field can pinpoint locations of different calling individuals using time-of-detection and direction of arrival (Dawson & Efford, 2009). Such data are analysed using spatially-explicit capture recapture models to provide more precise estimate densities (Dawson & Efford, 2009). However, microphone arrays may be impractical for wide-scale deployments and costly (Pérez-Granados & Traba, 2021). Additionally, both methods are not designed to estimate abundances of large aggregations of birds. Several studies have used number of vocalizations per recording time (i.e. call rate) as a predictor for abundance or density typically in a general linear model (e.g. Borker et al., 2014; Kloepper et al., 2016). However, such methods are less reliable in estimating large communally roosting birds where several hundreds or even thousands of individuals are vocalizing in unison.

In this study, we estimated the communal roost size of the Javan myna (*Acridotheres javanicus*), in Singapore using passive acoustic recorders and analysed the roost chorus in Singapore by applying machine learning methods. Javan mynas are an invasive bird species in Singapore and roost communally in trees with dense canopies sometimes numbering in the thousands near

anthropogenic food sources (Lim et al., 2003; Yap & Sodhi, 2004). They emit a loud and incessant roost chorus that can be intolerable to some residents that live in the vicinity of the roosts (Yap et al., 2002). While sound intensity has previously been used to estimate roost sizes (e.g. Sandoval et al., 2023), it is also affected by various factors such as distance to the recorder, urban conditions (e.g. buildings and street trees), weather conditions, and noise from other sources. Hence, we developed a novel approach and explored machine learning techniques that implicitly extract higher order statistical information from the sound recordings with a neural network, and use those to estimate the roost sizes of the Javan mynas.

2 | METHODS

2.1 | Video analysis technique

To develop an acoustic technique to estimate myna roost sizes, we had to ground truth the number of roosting mynas to calibrate our acoustic model. To achieve this, we developed an automated

visual technique to count mynas flying in and out of a roost site early in the evenings, before mynas start arriving at the site. The difference between the cumulative number of mynas arriving at the site and leaving the site was the number of mynas at the roost site.

While manually counting mynas coming in and out of a roost site is possible, it is error prone and labour intensive. We therefore focused on the development of an automated visual technique based on analysis of video recordings from two cameras pointed at the roost tree from different angles. The two cameras together provided a full view of the tree from all angles, so all arriving and leaving mynas could be counted. Addtionally, we validated the technique by manually counting the mynas in one set of video recordings and compared it against the visual automated analysis.

We chose a roost tree that was separated from nearby trees (i.e. non-joining canopies) and other nearby occlusions, such that we could see mynas coming in and out of the tree from all directions (roost tree 1 in Figure 1a). Two cameras were deployed facing the tree from about 1–2 h before sunset, until well after sunset. This covers the time during which the mynas arrive at the tree, and lasts until the end of the acoustic measurements that we compare the cameras counts against. Camera 1 was usually set up on the south-east of the tree, and Camera 2 on the north-west (Figure 1a). We collected multiple datasets from the same roost site on different days, at different times of the year (Table 1).

To automate our detection of birds flying in and out of the roost site, we drew boundaries around the tree, and counted birds crossing the boundaries in either direction. We call these boundaries "virtual markers" (Figure 1). Whenever a bird crossed a marker, we estimated its direction of flight and determined if it was flying in or out and updated the estimated bird count at the roost site (Figure 1b,c).

Detecting dark birds against a light sky background (even in twilight hours with sufficient light) was reliably achieved with simple image processing techniques. We used a rapid change in brightness of pixels on the marker for bird detection. We added a minimum required time gap between detections in the same location in the image to avoid duplicate detections from the same bird flapping its wings or moving in a way that causes the brightness to oscillate as the bird crossed the marker.

While two cameras ensured that we had complete view of the roost tree to see birds arriving from all directions, it also posed a challenge. A single bird might be seen on both cameras and could be double counted as shown in Figure 1b. Birds crossing the marker from the south-west or north-east could be potentially detected on both cameras. To avoid double-counting, we had to associate detections from both cameras and only count detections on one of the cameras. This was achieved with heuristics such as proximity in time, detection on opposite boundaries on the two cameras, and direction of flight. The dataset collected on 3 September 2020 was used as the primary dataset for validation of the visual analysis technique (Table 1). For this dataset, we performed manual counting of birds by carefully watching videos from both cameras and annotating the arrival and departure of each bird.

2.2 | Acoustic recording analysis technique

The audio dataset collected on 3 September 2020 was used as *training data* in our acoustic analysis. An acoustic recorder was set up close to Camera 1 during data collection. The exact locations of the cameras and the acoustic recorder differed on different days, as the intent was to make the techniques robust against small differences in the recorder setup. Both cameras and the acoustic recorder were synchronized in time.

The audio data was collected using a Zoom H6 recorder and an Electro-Voice ND66 condenser cardioid instrument microphone (Figure S1). The directional microphone was mounted on a tripod and placed about 5–10 m from the roost tree of interest and pointed into the centre of the foliage of the tree. The acoustic technique developed is not sensitive to the exact distance, as long as the roost chorus is audible at the microphone and the roost does not span more than a 90° angle from the microphone. The microphone has a beamwidth of about 90°, which was sufficient to cover the roost site, but not so wide as to pick up significant noise from other nearby roost sites.

In the time series of the recorded data, the sound intensity increased as the roost chorus got louder through the evening (Figure S2). The sudden drop in intensity at the 1 h 24-min mark occurred during a disturbance, and then gradually increased as the birds returned to their roost. After sunset, the roost chorus gradually fades till the birds stop vocalizing. Several loud events also can be observed throughout the recording, representing noises that are inevitable when recording in uncontrolled settings and public places.

While the data at first glance suggested we could use the acoustic timeseries amplitude to estimate roost sizes, it can be confounded by multiple factors. These include the distance between the roost site and the recorder, the environmental acoustic propagation conditions, the local noise sources, the gain settings on the recorder, the pointing direction of the microphone. Thus, the timeseries amplitude might not represent a close proxy of roost size since these variables were difficult to control operationally. As such, we considered other properties of the acoustic timeseries in our analysis.

2.3 | Machine learning

A traditional approach to finding acoustic timeseries properties of interest would be to handcraft *features* based on temporal statistics of the timeseries data. Such features often include ratios of power spectral densities at various frequencies, and other higher-order temporal statistics. These handcrafted features can then be used for regression analysis to calibrate a model. Here, we applied a deep neural network (DNN) to *learn* the features from the timeseries data.

Before feeding the timeseries data to a DNN, we decided to bandpass filter the data to remove frequencies that were dominated by traffic and other urban sounds, and did not contain much roost chorus. Since the roost chorus was mostly in the 1–5 kHz band (Figure S2), we applied a digital finite impulse response (FIR)

SOH ET AL.

Ecological Solutions
and **Evidence**

BRITISH
ECOLOGICAL
SOCIETY

5 of 10

bandpass filter (with 128 taps) to remove other sounds. The recording was then down sampled at 16,384 Hz, well above Nyquist frequency, to reduce the number of timeseries samples in the recording. The recorded time series was then split into 4096 sample blocks (250 ms blocks) and used as input to the DNN.

The architecture of the DNN is shown in Figure 2a. We used a 1D convolutional DNN with three convolutional layers, one mean pooling layer, followed by three dense fully-connected layers in the DNN, working directly with the acoustic data at the input. This is quite different from common approaches in DNN, where the data is first converted to a 2D spectrogram image and fed to a 2D convolutional DNN designed to work with images. Here, the 2D spectrogram conversion was unnecessary, and potentially detrimental to the retention of information in the acoustic recording as spectrogram conversion loses phase information from the original time series data. We used a normalization layer at the input of the DNN, removing any cues on acoustic intensity, as we did not want the DNN to learn to use the relationship with intensity for roost size estimation. While the relationship with intensity was strong, it was unreliable due to factors discussed earlier. We used a scaling layer at the output of the DNN to convert a normalized output to a scale that is relevant to typical roost sizes. This scaling was determined based on the roost size estimates from the video analysis of the same dataset. Appropriate scaling aids in training of the DNN and can be considered a hyperparameter of the model, but is not required to be very accurate; we only needed to know the rough order of magnitude roost size to choose the scale.

To train the network, we used a backpropagation-based learning algorithm (ADAM) with a learning rate of 0.002, early stopping, and a mini-batch size of 128 samples. This learning rate, as well as the DNN architecture, was obtained through many hyper-parameter optimization runs. We used 85% of the available 250 ms blocks as training samples, and the remaining 15% as validation samples. Furthermore, we augmented the training data with four weakly filtered (2-tap finite impulse response filters with weights [1.0, ±1.0] and [1.0, ±0.5]) versions of the input data. The augmentation helped to improve robustness of the DNN to changes in environmental

acoustic propagation and noise conditions. The trained DNN was saved to disk for use in an acoustic roost size estimation model described next.

2.4 | Acoustic roost size estimation model

The trained DNN from the previous section formed the heart of the acoustic roost size estimation model outlined in Figure 2b. In order to estimate the roost size, we bandpass filtered the acoustic recording in the 1–5 kHz band and split it into 1-min blocks. We then further split each 1-min block into 250 ms chunks, as we did during training. These chunks were fed to the trained DNN, and the bird count estimates from each 1-min block were statistically pooled to yield a median estimate and a 50% confidence interval. The process was repeated for each 1-min block to yield a timeseries of bird count estimates. The largest bird count during an evening of data collection could then represent our roost size estimate.

2.5 | Analysis of different data sets for model validation

We first developed an acoustic roost size estimation model based on training data recorded on 3rd September 2020 (Table 1). We tested this model with datasets recorded at the same roost site on other days, months later, and also on datasets recorded at other roost sites to demonstrate the robustness of the trained model.

The primary dataset we used for validating our acoustic roost size estimation model was a dataset collected on 17 February 2021, about 5 months after the training dataset (Table 1). While we collected this dataset at the same location, a lot had changed between the two collections. The seasons had changed, the trees were pruned, the acoustic recorder was set up at a different location and a different directional microphone was used. So, for all practical purposes, this acoustic dataset was independent of the dataset collected on 3rd September 2020.
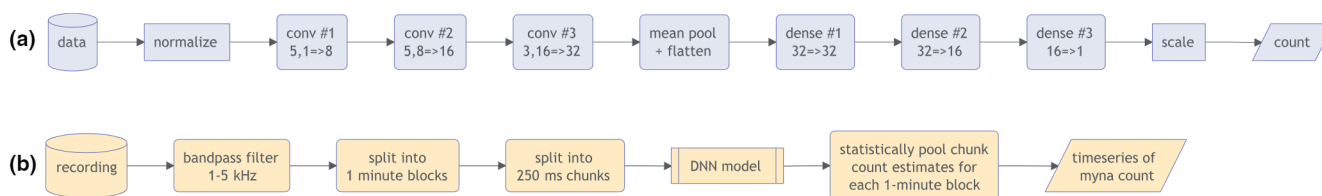
FIGURE 2 (a) Deep neural network (DNN) architecture to convert acoustic data to myna count. The input data size is 4096 samples (250 ms) of acoustic data at a sampling rate of 16,384 Hz. Each convolution layer down samples with a stride of 2, while increasing the number of filters from 1→8→16→32. The data from the 32 filters is mean-pooled, flattened and passed through 2 dense hidden layers with 32 and 16 neurons each, and then fed into an output dense layer with a single neuron. The output of that neuron is finally scaled to give the myna count estimate. (b) Complete processing chain from acoustic recording to timeseries of myna count estimates. The recording is bandpass filtered in the 1–5 kHz band and then split into 1-min blocks, and further split into 4096 sample (250 ms) chunks. Each 4096 sample chunk passes through the DNN (detailed in part a) to yield a point myna count estimate. The count estimates are statistically pooled over each 1-min block to yield a timeseries of median and a 50% confidence interval.

To further validate the acoustic model, we presented data from yet another dataset collected at the same roost site on 20 August 2020, about 2 weeks before the training data was collected (Table 1). This dataset, unfortunately, had a problem with the microphone cable after about 18 min, and so the comparison can only be made until then. Data from a different roost site (site 2) was collected on 31 August 2020 (Table 1). The site did not permit full visual analysis due to occlusions on one side of the roost tree. However, camera recordings were made to provide a rough visual estimate.

We also collected a dataset on 5 February 2021, but it was very windy. To reduce wind noise, we put on a wind cover (foam cover) on the microphone during the data collection (Table 1). Later, it was clear that it sounded more muffled than the usual recordings. A spectral analysis of the recording showed that the high frequency sounds were significantly attenuated in this recording. To test the robustness of the acoustic model, we processed this recording using the acoustic roost size estimation model and compared it with the estimates from visual analysis of camera recordings.

3 | RESULTS

3.1 | Video analysis

Our manual counts agree closely (within 5%) with the counts from the automated visual analysis in Figure S3, and we use visual analysis for other datasets. The sudden dip in bird count at about 86 min corresponds to an event when the birds seemed to have been *scared* by something, and many flew out of the tree. A manual visual check of the video at that time confirmed this and the audio recordings at that time also clearly showed a disturbance. The birds came back within a few minutes and continued their roost chorus. Such sudden departures were a common occurrence, as seen in many of our datasets. There was significant variability in the number of birds at the roost across days, especially between the 2020 datasets and the 2021 datasets (separated by 5 months; Figure S4). The differences were consistent with the acoustic recording analysis as seen later and may be potentially attributed to pruning of the trees between the two data collection windows.

3.2 | Acoustic analysis

The acoustic model results matched the visual analysis results closely, suggesting that roost size estimates can be obtained from the acoustic data alone. The roost size estimate was the maximum acoustic estimate during the entire dataset, which was close to 400 birds for this roost.

The same dataset was used in training the acoustic model, and in evaluating its efficacy (Figure 3a). Although we separated the training data from the validation data, as is the norm in machine learning, both data came from the same day's recording (same dataset recorded on 3rd September 2020). The correlation coefficient (*r*) between the acoustic and visual estimates is 0.978 with a root mean square error (RMSE) of 26.8 (6% of the roost size). Next, we see that the acoustic roost size estimation model performed robustly with datasets recorded on other days as well—even datasets collected months later.
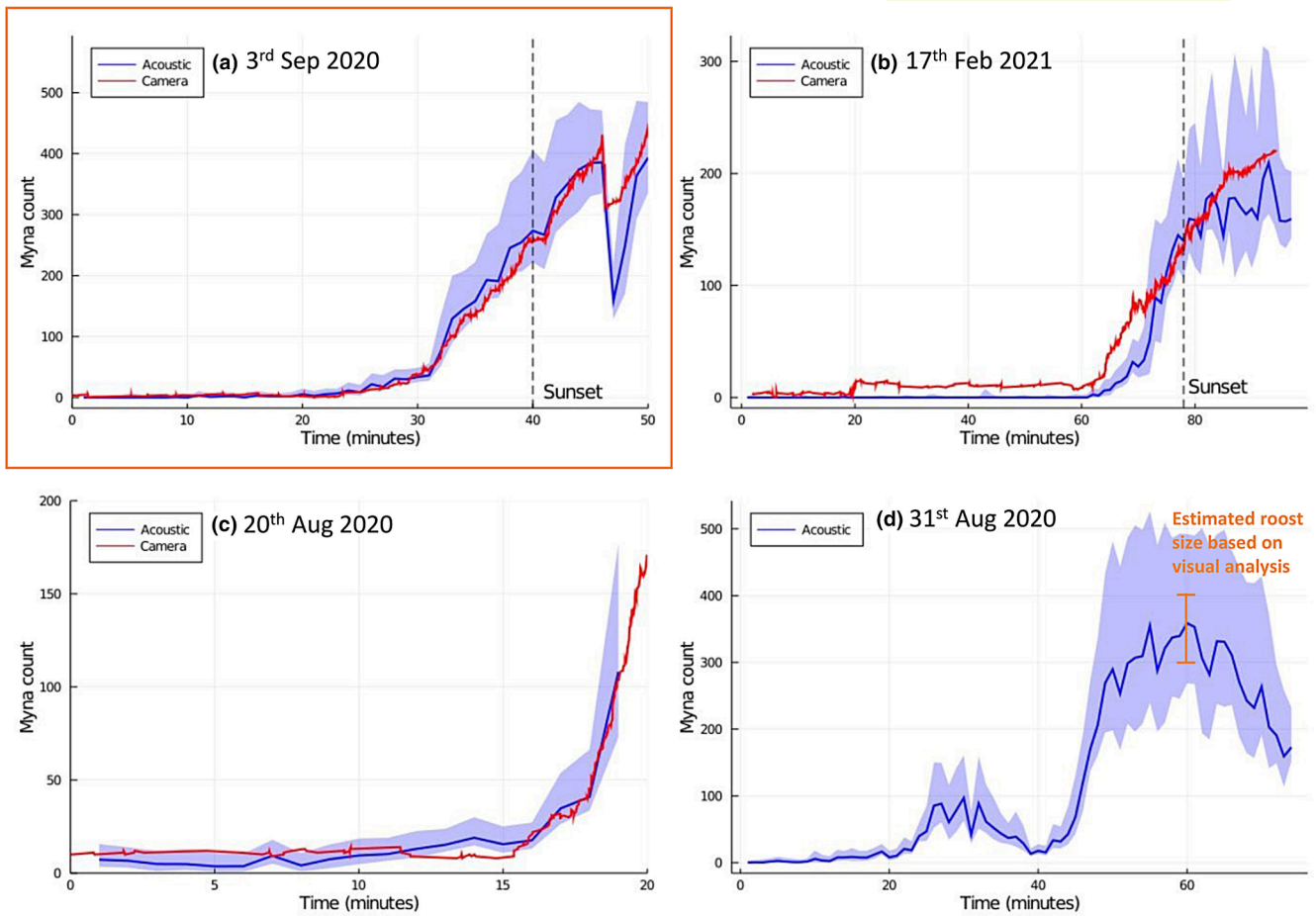
3.3 | Validation using different data sets

Figure 3b shows the time evolution of estimated bird count based on the acoustic roost size estimation model, as compared with the estimate from visual analysis using two cameras for the same dataset collected on 17 February 2021. The roost estimate is about 210 birds and the match between the acoustic and visual models was close (*r*=0.981, RMSE=18.4; 8% of roost size). This suggests that the acoustic model is suitable for use in estimation of myna roost sizes, without the need for the visual camera-based analysis to be undertaken at other sites. Also, the acoustic model matched the visual results closely at the same roost site with recordings collected on a different date, 20 August 2020 (*r*=0.795, RMSE=5.6; 6% of roost size; Figure 3c).

For site 2 data collected on 31 August 2020, our rough visual analysis provided an order of magnitude estimate of the roost size to be 300–400 birds. Based on the acoustic model, the roost size was about 350 birds, consistent with the rough visual analysis (Figure 3d).

If a windshield was added to our microphone, the acoustic model underestimated the number of birds at any given time since the recording had a significantly different frequency response than the training data (left panel of Figure S5). On re-calibrating the model for the difference (re-calibration requires availability of visual estimates), we attained accurate results from the model, even with the modified frequency response (right panel of Figure S5).

4 | DISCUSSION

We conclude that the use of passive acoustic recordings of myna roost chorus to estimate large roost sizes is indeed feasible, and we have developed acoustic techniques to do this robustly using a simple portable acoustic recording system consisting of a tripod, digital recorder coupled with a directional microphone. We validated the machine-learning based acoustic techniques developed using an automated visual analysis with a dual-camera setup and with manual bird counting. We also showed that the acoustic roost size estimation technique developed attained accurate roost estimates on different datasets, if the equipment used is similar. If the microphone frequency response is significantly different, the technique requires a re-calibration for accurate results. In practice, one has to calibrate

FIGURE 3 (a) Myna count estimates (median) from acoustic roost size estimation model ("Acoustic" in blue) as a function of time, compared against the estimates from visual analysis ("Camera" in red). The light blue ribbon is the 50% confidence interval from the model. Orange outline shows the count estimation using the training data while the other plots are representative of validation data. (b) Temporal evolution of estimated bird count based on the acoustic roost size estimation model, as compared with the estimate from visual analysis, for test datasets collected on 17 September 2021, (c) 20 August 2020 and (d) 31 August 2020 at roost site 2—a rough visual estimate of the roost size is provided since part of the roost tree was occluded with foliage from another tree.

the technique for a chosen equipment. Once calibrated, equipment type changes should be avoided, and if they become necessary, a re-calibration should be performed.

The video analysis technique presented was suited for datasets where the roost tree is clearly separated from nearby trees and buildings. This is required to construct a virtual marker around the tree, and to ensure that birds coming in and out from all directions are visible on at least one of the two cameras. While this technique alone may be sufficient to estimate roost sizes for some roosts, it is logistically challenging to collect the required video data, and many roost sites do not lend themselves to the visual separation needed for this technique to work. Hence, our acoustic method is more widely applicable given the many logistical constraints that rely on visual or weather radar methods to infer population estimates. Visual counts are manpower intensive and time consuming as several surveyors are needed to count birds prior to roosting and radar data are not suited for accurately estimating smaller roost sizes.

Nonetheless, there are some limitations in our acoustic application to estimate the number of communal roosting birds. Firstly, not all communal roosts are occupied by a single species. For example, Javan mynas and common mynas (*Acridotheres tristis*) often share the same roost tree. In this instance, monitoring the roost populations of both species collectively may be sensible management-wise since they are invasive and commonly roost in trees near residential areas causing dis-amenities (Lim et al., 2003). Moreover, they are closely related, of similar size and their calls are almost indistinguishable even to seasoned bird watchers. However, our method may be less suited in estimating populations of threatened species or species of a particular interest if they roost with other species.

There are further considerations using roosts to infer population estimates. For one, it is assumed that all roost locations within a geographic area of interest are known, which is more attainable in smaller or isolated areas. Additionally, not all individuals in the population may be roosting communally and roost sizes can also vary temporally; if so, other methods should be considered. For non-migratory species, breeding adults typically roost away from communal roost sites thus population estimates at their roosts should ideally be conducted during the non-breeding season (Saldanha

et al., 2019). However, for some migratory species, roost estimates in their wintering grounds may provide a fairer reflection of their population.

All in all, our approach provides less laborious and a more reliable method for estimating and monitoring changes in avian roost populations than previous approaches. Possible ecological applications include monitoring roost site fidelity, population responses to habitat loss or degradation and testing the efficacy of management measures such as roost tree pruning to reduce undesirable roost populations. While our model was developed for primarily gregarious roosting birds, our approach with further testing, could be adapted to estimate populations of other wildlife that also congregate such as communally roosting bats and insect aggregations (e.g. locust swarms, and temporary aggregations of crickets and cicadas).

AUTHOR CONTRIBUTIONS

ACKNOWLEDGEMENTS

CONFLICT OF INTEREST STATEMENT

The authors declare no conflict of interest.

PEER REVIEW

The peer review history for this article is available at https://www.webofscience.com/api/gateway/wos/peer-review/10.1002/2688-8319.12394.

DATA AVAILABILITY STATEMENT

Data and code available from the Dryad Digital Repository https://doi.org/10.5061/dryad.12jm63z77 (Chitre et al., 2024).

ORCID

Malcolm C. K. Soh https://orcid.org/0000-0002-9490-147X
Mandar A. Chitre https://orcid.org/0000-0001-6243-7871
Matthias Hoffmann-Kuhnt https://orcid.org/0000-0001-9533-1248
Benjamin P. Y.-H. Lee https://orcid.org/0000-0002-9952-1011
Kenneth B. H. Er https://orcid.org/0000-0003-4485-7260

REFERENCES

Beauchamp, G. (1999). The evolution of communal roosting in birds: Origin and secondary losses. *Behavioral Ecology, 10*(6), 675–687. https://doi.org/10.1093/beheco/10.6.675

Bombaci, S. P., & Pejchar, L. (2019). Using paired acoustic sampling to enhance population monitoring of New Zealand's forest birds. *New Zealand Journal of Ecology, 43*(1), 3356.

Borker, A. L., McKown, M. W., Ackerman, J. T., Eagles-Smith, C. A., Tershy, B. R., & Croll, D. A. (2014). Vocal activity as a low cost and scalable index of seabird colony size. *Conservation Biology, 28*(4), 1100–1108. http://www.jstor.org/stable/24480088

Brodsky, L. M., & Weatherhead, P. J. (1984). Behavioural thermoregulation in wintering black ducks: Roosting and resting. *Canadian Journal of Zoology, 62*(7), 1223–1226. https://doi.org/10.1139/z84-177

Burger, J. (1983). Bird control at airports. *Environmental Conservation, 10*(2), 115–124. https://doi.org/10.1017/S0376892900012200

Chabot, D., & Francis, C. M. (2016). Computer-automated bird detection and counts in high-resolution aerial images: A review. *Journal of Field Ornithology, 87*(4), 343–359. https://doi.org/10.1111/jofo.12171

Cheke, R. A., & El Hady Sidatt, M. (2019). A review of alternatives to fenthion for quelea bird control. *Crop Protection, 116*, 15–23. https://doi.org/10.1016/j.cropro.2018.10.005

Chitre, M. A., Hoffmann-Kuhnt, M., Soh, M. C. K., Lee, B. P. Y.-H., & Er, K. B. H. (2024). A novel method for estimating avian roost sizes using passive acoustic recordings. *Dryad Digital Repository.* https://doi.org/10.5061/dryad.12jm63z77

Clark, B. A., Klug, P. E., Stepanian, P. M., & Kelly, J. F. (2020). Using bioenergetics and radar-derived bird abundance to assess the impact of a blackbird roost on seasonal sunflower damage. *Human-Wildlife Interactions, 14*(3), 427–441. https://www.jstor.org/stable/27316221

Cougill, S., & Marsden, S. J. (2004). Variability in Roost Size in an Amazona Parrot: Implications for Roost Monitoring/Variabilidad en el tamaño de los dormideros de una Amazona: implicaciones para el monitoreo de dormideros. *Journal of Field Ornithology, 75*(1), 67–73. http://www.jstor.org/stable/4151245

Dawson, D. K., & Efford, M. G. (2009). Bird population density estimated from acoustic signals. *Journal of Applied Ecology, 46*(6), 1201–1209. https://doi.org/10.1111/j.1365-2664.2009.01731.x

Deepe, G. S., Jr. (2018). Outbreaks of histoplasmosis: The spores set sail. *PLoS Pathogens, 14*(9), e1007213. https://doi.org/10.1371/journal.ppat.1007213

Deng, Y., Belotti, M. C. T. D., Zhao, W., Cheng, Z., Perez, G., Tielens, E., Simons, V. F., Sheldon, D. R., Maji, S., Kelly, J. F., & Horton, K. G. (2023). Quantifying long-term phenological patterns of aerial insectivores roosting in the Great Lakes region using weather surveillance radar. *Global Change Biology, 29*(5), 1407–1419. https://doi.org/10.1111/gcb.16509

Denton, J. F., & Di Salvo, A. F. (1968). The prevalence of Cryptococcus neoformans in various natural habitats. *Sabouraudia: Journal of Medical and Veterinary Mycology, 6*(3), 213–217. https://doi.org/10.1080/00362176885190411

Dolbeer, R. A. (1990). Ornithology and integrated pest management: Red-winged blackbirds *Agelaius phoeniceus* and corn. *Ibis, 132*(2), 309–322. https://doi.org/10.1111/j.1474-919X.1990.tb01048.x

Giunchi, D., Albores-Barajas, Y. V., Baldaccini, N. E., Vanni, L., & Soldatini, C. (2012). Feral pigeons: Problems, dynamics and control methods. In *Integrated pest management and pest control. current and future tactics* (pp. 215–240). InTechOpen.

Goodenough, A. E., Little, N., Carpenter, W. S., & Hart, A. G. (2017). Birds of a feather flock together: Insights into starling murmuration behaviour revealed using citizen science. *PLoS One, 12*(6), e0179277. https://doi.org/10.1371/journal.pone.0179277

Gregory, R. D., Gibbons, D. W., & Donald, P. F. (2004). Bird census and survey techniques. In W. J. Sutherland, I. Newton, & R. Green (Eds.), *Bird ecology and conservation* (pp. 17–56). Oxford University Press.

SOH ET AL.

Ecological Solutions
and Evidence

BRITISH
ECOLOGICAL
SOCIETY

9 of 10

Gurney, J. W., & Conces, D. J. (1996). Pulmonary histoplasmosis. *Radiology*, *199*(2), 297–306. https://doi.org/10.1148/radiology.199.2.8668768

Haag-Wackernagel, D., & Geigenfeind, I. (2008). Protecting buildings against feral pigeons. *European Journal of Wildlife Research*, *54*(4), 715–721. https://doi.org/10.1007/s10344-008-0201-z

IUCN. (2022). The IUCN Red List of Threatened Species. Version 2022-2. https://www.iucnredlist.org

Kloepper, L. N., Linnenschmidt, M., Blowers, Z., Branstetter, B., Ralston, J., & Simmons, J. A. (2016). Estimating colony sizes of emerging bats using acoustic recordings. *Royal Society Open Science*, *3*(3), 160022. https://doi.org/10.1098/rsos.160022

Lichtenwalter, C., Steensma, K., Marcondes, M., Taylor, K., McConnel, C., & Adams Progar, A. (2023). Seasonal use of dairies as overnight roosts by common starlings (*Sturnus vulgaris*). *Birds*, *4*, 213–224. https://doi.org/10.3390/birds4020018

Lim, H. C., Sodhi, N. S., Brook, B. W., & Soh, M. C. K. (2003). Undesirable aliens: Factors determining the distribution of three invasive bird species in Singapore. *Journal of Tropical Ecology*, *19*(6), 685–695. http://www.jstor.org/stable/4091842

Malik, R., Krockenberger, M. B., Cross, G., Doneley, R., Madill, D. N., Black, D., Mcwhirter, P., Rozenwax, A., Rose, K., Alley, M., Forshaw, D., Russell-Brown, I., Johnstone, A. C., Martin, P., O'Brien, C. R., & Love, D. N. (2003). Avian cryptococcosis. *Medical Mycology*, *41*(2), 115–124. https://doi.org/10.1080/mmy.41.2.115.124

Marzluff, J. M., Heinrich, B., & Marzluff, C. S. (1996). Raven roosts are mobile information centres. *Animal Behaviour*, *51*(1), 89-103.

Matuzak, G. D., & Brightsmith, D. J. (2007). Roosting of yellow-naped parrots in Costa Rica: Estimating the size and recruitment of threatened populations. *Journal of Field Ornithology*, *78*(2), 159–169. https://doi.org/10.1111/j.1557-9263.2007.00099.x

Merola-Zwartjes, M. (1998). Metabolic rate, temperature regulation, and the energetic implications of roost nests in the Bananaquit (*Coereba flaveola*). *The Auk*, *115*(3), 780–786. https://doi.org/10.2307/4089429

Pérez-Granados, C., & Traba, J. (2021). Estimating bird density using passive acoustic monitoring: A review of methods and suggestions for further research. *Ibis*, *163*(3), 765–783. https://doi.org/10.1111/ibi.12944

Russell, K. R., & Gauthreaux, S. A. (1998). Use of weather radar to characterize movements of roosting purple martins. *Wildlife Society Bulletin (1973–2006)*, *26*(1), 5–16. http://www.jstor.org/stable/3783794

Saldanha, S., Taylor, P. D., Imlay, T. L., & Leonard, M. L. (2019). Biological and environmental factors related to communal roosting behavior of breeding bank swallow (*Riparia riparia*). *Avian Conservation and Ecology*, *14*(2), 21. https://doi.org/10.5751/ACE-01490-140221

Sandoval, N., Denyer, K., Dowling, S., Barot, D., & Fan, N. (2023). Testing the effectiveness of a novel approach to measure a large roosting congregation in a wetland ecosystem. *New Zealand Journal of Ecology*, *47*(1), 3513. https://doi.org/10.20417/nzjecol.47.3513

Van Den Broeke, M. S. (2019). Radar quantification, temporal analysis and influence of atmospheric conditions on a roost of American robins (*Turdus migratorius*) in Oklahoma. *Remote Sensing in Ecology and Conservation*, *5*(2), 193–204. https://doi.org/10.1002/rse2.99

van Els, P., & van Turnhout, C. (2021). *Communal roost counts in the netherlands: A summary of 10 years of monitoring*. 343, 3–8.

Van Wilgenburg, S., Solymos, P., Kardynal, K., & Frey, M. (2017). Paired sampling standardizes point count data from humans and acoustic recorders. *Avian Conservation and Ecology*, *12*, 13. https://doi.org/10.5751/ACE-00975-120113

Wang, S., & Chu, L. M. (2021). Microhabitat characteristics related to seasonal roost switching: Implications from a threatened and introduced cockatoo species in an urban landscape. *Avian Research*, *12*(1), 35. https://doi.org/10.1186/s40657-021-00270-9

Ward, P., & Zahavi, A. (1973). The importance of certain assemblages of birds as "information-centres" for food-finding. *Ibis*, *115*(4), 517–534. https://doi.org/10.1111/j.1474-919X.1973.tb01990.x

Yap, C. A. M., & Sodhi, N. S. (2004). Southeast Asian invasive birds: Ecology, impact and management. *Ornithological Science*, *3*(1), 57–67. https://doi.org/10.2326/osj.3.57

Yap, C. A. M., Sodhi, N. S., & Brook, B. W. (2002). Roost characteristics of invasive mynas in Singapore. *The Journal of Wildlife Management*, *66*(4), 1118–1127. https://doi.org/10.2307/3802943

Yip, D. A., Knight, E. C., Haave-Audet, E., Wilson, S. J., Charchuk, C., Scott, C. D., Sólymos, P., & Bayne, E. M. (2020). Sound level measurements from audio recordings provide objective distance estimates for distance sampling wildlife populations. *Remote Sensing in Ecology and Conservation*, *6*(3), 301–315. https://doi.org/10.1002/rse2.118

Zulian, V., Müller, E. S., Cockle, K. L., Lesterhuis, A., Tomasi Júnior, R., Prestes, N. P., Martinez, J., Kéry, M., & Ferraz, G. (2020). Addressing multiple sources of uncertainty in the estimation of global parrot abundance from roost counts: A case study with the Vinaceous-breasted parrot (*Amazona vinacea*). *Biological Conservation*, *248*, 108672. https://doi.org/10.1016/j.biocon.2020.108672

SUPPORTING INFORMATION

Additional supporting information can be found online in the Supporting Information section at the end of this article.

Figure S1. Zoom H6 acoustic recorder and Electro-Voice ND66 condenser cardioid instrument microphone used for all audio recordings analysed in this report and the field set up (right panel).

Figure S2. Above: Time series of the recorded acoustic data for dataset collected on 3rd September 2020. The x-axis is time (hours), relative to start of recording, and the y-axis is proportional to the acoustic pressure measured by the microphone. The acoustic pressure is uncalibrated and −1 to 1 is the full dynamic range. Below: Spectrogram of the recorded acoustic dataset collected on 3rd September 2020 using an 8192 sample window. The x-axis is time (hours), relative to start of recording, and the y-axis is the acoustic frequency in Hz. The colour corresponds to the acoustic intensity at a given time and frequency, with darker red-orange colours indicating higher intensity.

Figure S3. A plot of number of birds at the roost site as a function of time using visual estimates only. The red curve is from automated visual analysis, whereas the blue curve is from manual counting. Both curves agree well. The sudden dip in bird count at about 86 min corresponds to an event when the birds seemed to have been *scared* by something, and many flew out of the tree, but returned within minutes.

Figure S4. Bird count estimates at roost site 1 from 4 different datasets, collected on 20th August 2020, 3rd September 2020, 5th February 2021 and 17th February 2021. Some variability is observed across days, but the most significant differences may be potentially attributed to pruning of the trees between the two data collection windows.

Figure S5. Time evolution of estimated bird count based on the acoustic roost size estimation model, as compared with the estimate from visual analysis, for the dataset collected on 5th February 2021 using a microphone with wind cover. (a) The acoustic model results are inaccurate due to the wind cover modifying the frequency response of the microphone. (b) However, the acoustic model results agree with the visual model more closely after re-calibration.